Magnetic Particle Separation in a Liquid Column Based on Magnetophoresis

Ingo Kuehne[1*], Nadine Philippin[1,2] and Alexander Frey[3]
[1] Heilbronn University of Applied Sciences, Kuenzelsau, BW, Germany
[2] Technical University of Munich, Chair of Physics of Electrotechnology, Munich, BY, Germany
[3] Augsburg Technical University of Applied Sciences, Augsburg, BY, Germany
[*]ingo.kuehne@hs-heilbronn.de

In this paper, the topic of separation of sinking particles in a stationary liquid column based on magnetophoresis is studied in depth. For this purpose, the fundamentals of magnetophoresis are presented at the beginning. Subsequently, the modeling of the stationary liquid column is discussed in detail. The simulation results illustrate the vertical separation due to gravity and show the field-assisted transient horizontal deflection of the particles. Thus, a flexible method for magnetic particle separation was verified by simulations.

***Keywords*—magnetophoresis, field-assisted particle manipulation, microfluidics**

I. Introduction

Manipulation, including the separation and sorting of particles, is of great relevance in the field of medical diagnostics or biological/chemical analysis. Nowadays, there is a whole range of processes that can essentially be divided into active and passive techniques. Fig. 1 shows an overview.

The works of *Pamme* [1] and *Sajeesh et al.* [2] provide a review of the various state of the art techniques. The present paper refers exclusively to the active separation and sorting process using magnetic fields, known as magnetophoresis.

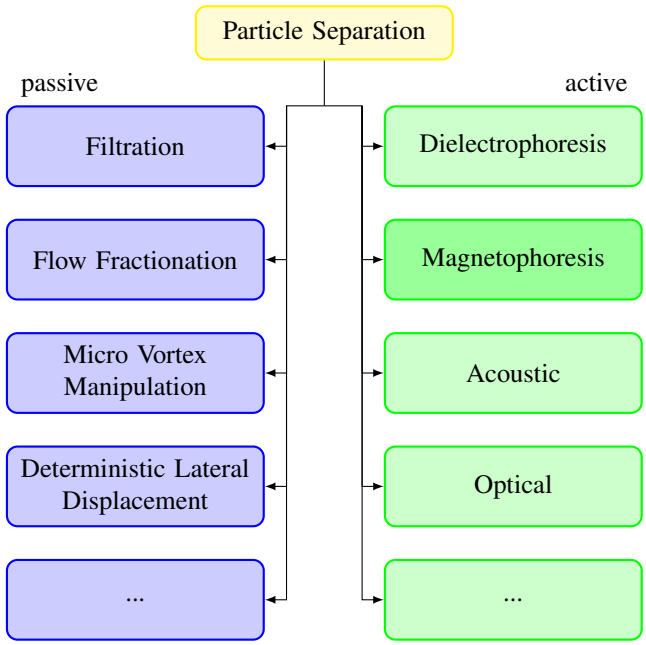

Fig. 1: Overview of separation techniques (adapted from [2]).

II. Magnetophoresis

Magnetophoresis is a phenomenon wherein charged or magnetically susceptible particles are selectively influenced by a magnetic field, resulting in their movement within a fluid medium. This process has garnered significant interest due to its potential applications in biomedical engineering, drug delivery, and environmental remediation.

The elementary work of *Rosensweig* [3] provided early insights into the behavior of magnetic fluids and the principles governing magnetophoresis.

This phenomenon exploits the magnetophoretic force, which is derived from the interaction between the magnetic moments of particles and the external magnetic field [4]. The magnetophoretic force F_m acting on a particle can be expressed as:

$$F_m = \frac{1}{4}\,\pi \cdot d^3 \cdot \mu_0 \cdot \mu_m \cdot K \cdot \nabla |H|^2 \tag{1}$$

where d is the diameter of the particle, μ_0 is the vacuum magnetic permeability, μ_m is the relative magnetic permeability of the medium, K is the Clausius-Mossotti factor and H is the applied magnetic field strength.

On the one hand, a distinction is made between positive magnetophoresis (*pM*). Here, paramagnetic particles in a diamagnetic fluidic medium are forced in the direction of high magnetic field strengths under the influence of a non-uniform magnetic field. On the other hand, there is negative magnetophoresis (*nM*), in which diamagnetic particles in a paramagnetic fluid are moved towards the minimum of an inhomogeneous magnetic field due to the different magnetic permeabilities. In this paper, reference is only made to the aspect of positive magnetophoresis.

The so-called Clausius-Mossotti factor K is the decisive variable that expresses the relationship between the particle and the surrounding liquid medium. In the case of *pM*, the corresponding value is positive; in the case of *nM*, it is negative. The Clausius-Mossotti factor is defined as:

$$K = \frac{\mu_p - \mu_m}{\mu_p + 2\,\mu_m} \tag{2}$$

with the relative magnetic permeability μ_p of the particle and μ_m of the fluidic medium.

For the sake of completeness, it should be noted that the magnetic permeability μ is a physical quantity that can be represented as a complex number [5]:

$$\mu = \mu^{'} - j\,\mu^{''} \tag{3}$$

with $\mu^{'}$ as the real part and $\mu^{''}$ as imaginary part. $\mu^{'}$ represents the ability of the material to store magnetic energy, while $\mu^{''}$ counts for the energy dissipation (e.g. core losses including hysteresis and eddy current losses). Consequently, the real part of the complex permeability can be related to inductance and the imaginary part to resistance.

Especially at high frequencies, the complex character of the magnetic permeability and thus also of the Clausius-Mossotti factor must not be neglected. In this paper, however, only DC magnetic fields are used, so that the frequency-dependent complex material behavior will not be taken into account.

III. Ferrite Powder

In this study, particles based on the manganese-zinc (MnZn) ferrite powder *2077* from TRIDELTA Weichferrite GmbH, Germany are examined in more detail [6]. First, the powder was examined in terms of particle size distribution. In a further step, the magnetic permeability was examined.

A. Particle Size Distribution

The processing of powders strongly depends on the particle size distribution (PSD). Ferrite powders, such as the present type *2077* are often a waste product in certain recycling processes and therefore usually have a wide range of particle sizes. Fig. 2 shows a first qualitative impression of the particle shape and size distribution.

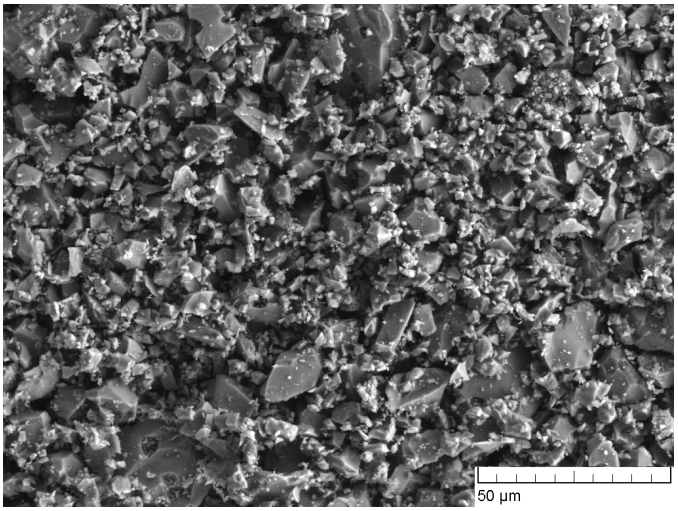

Fig. 2: SEM image of MnZn ferrite powder (TRIDELTA, type *2077*).

At first glance, a rather sharp-edged, uneven particle shape and a broad size distribution can be observed. The PSD was created quantitatively on the basis of a scanning electronic micorscopic (SEM) analysis of the powder. Fig. 3 presents a SEM image of the powder and the measurement of the particle diameters.

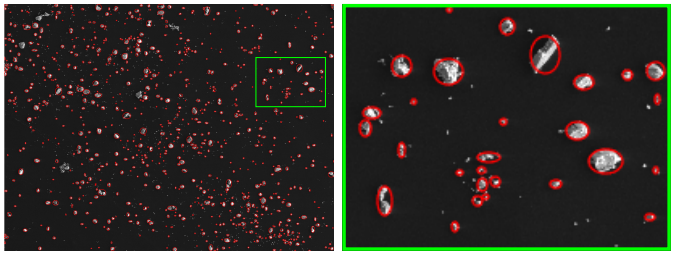

(a) (b)

Fig. 3: Particle size evaluation: (a) SEM evaluation of the particle diameter, and (b) detailed view of image analysis.

An image analysis using a Matlab script was used to calculate a histogram for the particle size distribution. Fig. 4 shows the PSD of the present ferrite powder.

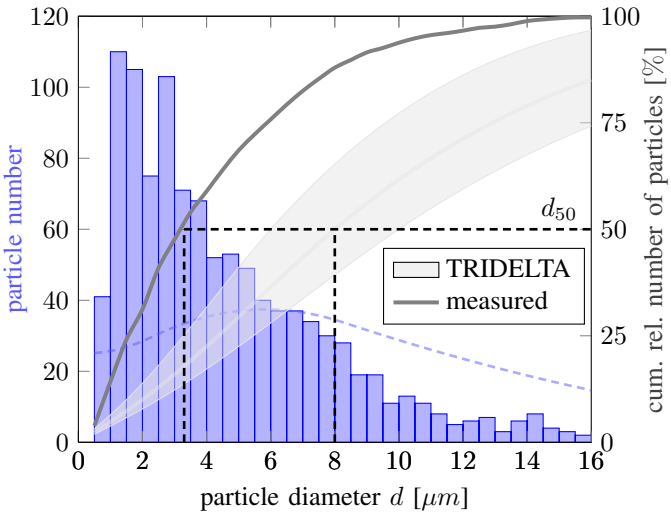

Fig. 4: Histogram of MnZn ferrite particle size distribution.

Important parameters for quantifying this statistical distribution are the 10%, 50% and 90% percentiles of the particle diameters (d_{10}, d_{50} and d_{90}) of the cumulative distribution. The *span*, respectively the distribution width, can be calculated from these values as follows:

$$span = \frac{d_{90} - d_{10}}{d_{50}} \tag{4}$$

Tab. I shows an overview of the statistical PSD values obtained.

TABLE I: Particle size distribution statistics.

	d_{10} [μm]	d_{50} [μm]	d_{90} [μm]	*span*
TRIDELTA [6]	2.0 ± 0.5	8.0 ± 2.0	30 ± 5	3.6 ± 0.3
SEM-measured	0.8	3.3	8.6	2.4

In comparison, it can be seen that the SEM-based measurement results in a narrower distribution with a smaller average particle diameter d_{50} than the manufacturer's specifications would suggest. This is most likely due to the powder preparation for the SEM examination, in which larger particles are less likely to adhere to the sample plate. However, our own measurements confirmed that powders exhibit a wide particle size distribution. This leads to problems during further processing, such as the clogging of printing nozzles or, as a result, to strongly fluctuating component properties (e.g. permeability of inductors).

It is therefore often necessary to design the particle sizes within a narrow range or to limit them to a maximum particle diameter. This is traditionally achieved by mechanical sieving, which is accompanied by several disadvantages, such as clogging of the sieves due to electrostatic charging.

For this reason, this paper presents an alternative ferromagnetic particle separation or rather sorting process based on the utilization of gravity and DC magnetic fields within a diamagnetic fluidic medium.

B. Magnetic Permeability

This MnZn ferrite powder of type *2077* is the base material for a wide range of inductive components, which are also used at higher frequencies. Therefore, the manufacturer provides extensive typical measured values for the frequency-dependent complex magnetic permeability (cf. Fig. 5).

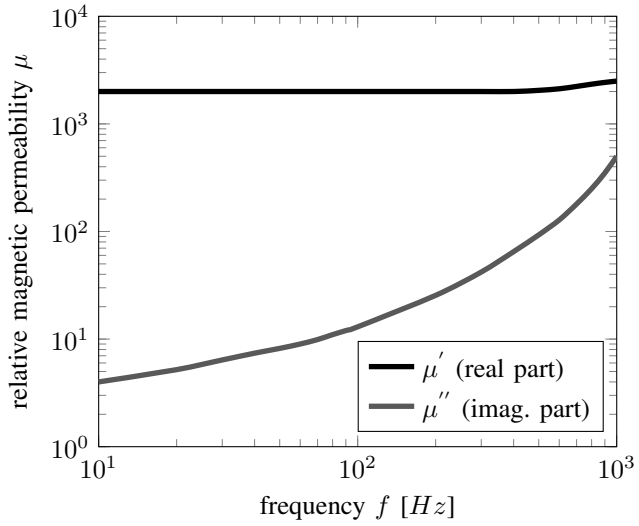

Fig. 5: Frequency-dependent relative magnetic permeability.

The expected Clausius-Mossotti factor can be easily calculated from these characteristic permeability values. Fig. 6 presents the frequency-dependent curve of the Clausius-Mossotti factor assuming that the diamagnetic liquid medium is water (cf. Tab. II).

It is easy to see that in this specific case and in this frequency range, the dominant real part of the Clausius-Mossotti factor is just under 1 and is almost independent of the frequency. The imaginary part of the Clausius-Mossotti factor is almost four orders of magnitude smaller and therefore negligible.

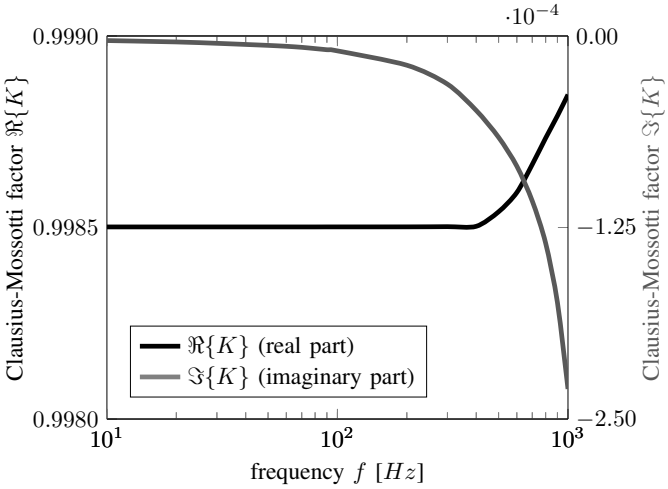

Fig. 6: Frequency-dependent Clausius-Mossotti factor.

Since this paper works with pure DC magnetic fields anyway, both the magnetic permeabilities and thus also the Clausius-Mossotti factor can be assumed to be constant.

IV. COMSOL Modeling

Using COMSOL, a geometric 2D model of a stationary separation column filled with a liquid was built up. In the upper section (surface of the liquid) is the inlet, where a certain amount of particles of different sizes are centrally and simultaneously fed to the separation column. The separation column itself consists of two sections. The upper section is used for vertical separation of particles of different sizes due to gravity. The lower section contains inductive coil arrays generating the DC magnetic field and is used for horizontal deflection of the particles based on magnetophoresis. At the bottom of the separation column are a left, middle and right separation zone to hold a respective size range of particles. Since only positive magnetophoresis is investigated here, i.e. the particles can only be deflected horizontally in the direction of the coil arrays. So, the right-hand separation zone is not relevant here. The separation zones could alternatively be designed as individual outlets.

The goal of the separation column is the defined reduction of the PSD span of the MnZn ferrite powder with the help of gravity and a time-dependent DC magnetic field. Fig. 7 illustrates the design of the separation column.

For this purpose, the simulation requires the physical COMSOL interfaces: *Magnetic Fields*, *Laminar Flow* and *Particle Tracing for Fluid Flow*. In a first study, the DC magnetic field distribution is investigated by means of a *Time-Domain* analysis. The time-dependent field consideration is necessary because the magnetic field is switched off after a defined period of time. The obtained results are the basis for a subsequent *Time-Domain* study for calculating the particle trajectories,

which is controlled by a time-dependent DC current I applied to the inductive coil arrays.

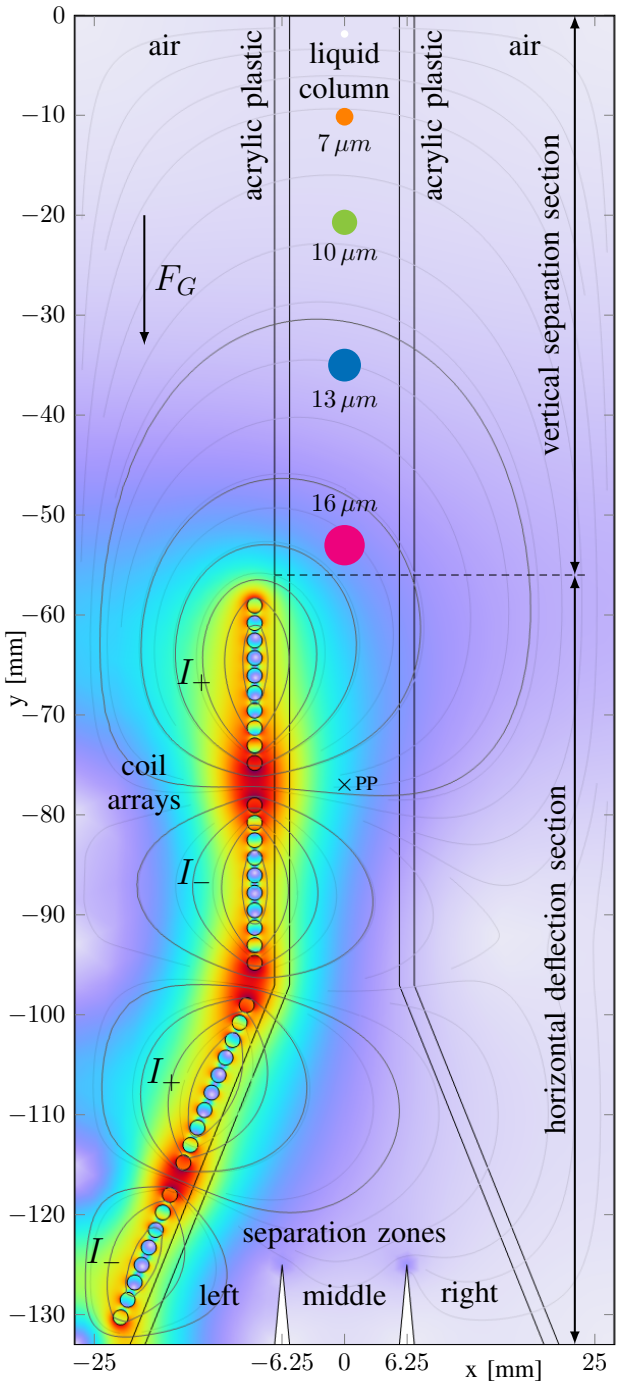

Fig. 7: Stationary liquid column with radius-dependent vertically separated particles (size scaled up for visibility) during a sink time of $t = 100s$.

All simulation results are based on the material properties of the present ferromagnetic MnZn particles of type *2077* sinking in pure water. Tab. II presents the material properties used in the simulation models.

TABLE II: Material properties.

	quantity	symbol	value	unit
fluidic medium (water)	density	ϱ_m	1,000	kg/m^3
	dyn. viscosity	η_m	1	$mPa\,s$
	rel. permeability	μ_m	1	–
particle (MnZn powder *2077*)	density	ϱ_p	4,800	kg/m^3
	rel. permeability[a]	μ_p	2,000	–

[a]Frequency-dependent complex function, see Fig. 5 .

V. Simulation Results

A. Vertical Separation

In the upper section, the particles are essentially subject to the balance of forces from gravitational force F_G, buoyancy F_A, and Stokes friction F_R in the fluid:

$$F_G = F_A + F_R \tag{5}$$

The force balance can easily be resolved analytically according to the sink velocity:

$$v = \frac{g \cdot (\varrho_p - \varrho_m)}{18\,\eta_m} \cdot d^2 \tag{6}$$

with g as acceleration of gravity, ϱ_p as particle density, ϱ_m as medium density and η_m as medium dynamic viscosity. The COMSOL-based simulation results visualized in Fig. 8 confirm the quadratic relationship between sink velocity and particle diameter.

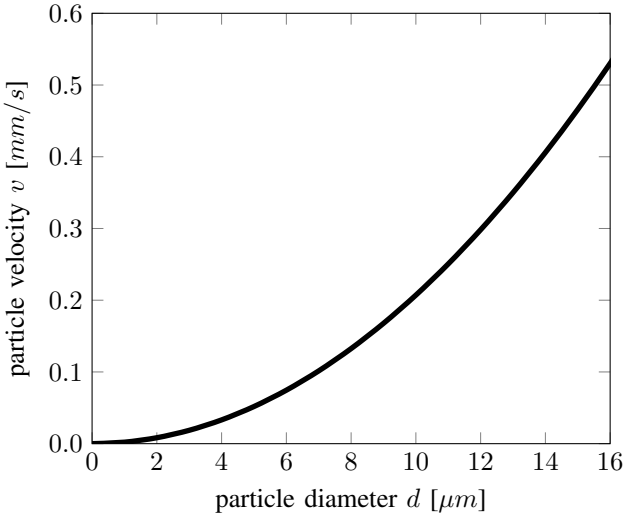

Fig. 8: Diameter-dependent particle velocity.

The sinking velocity of the particles has a decisive influence on the duration of a potential experiment. Particles with a diameter of 8µm, for example, already take a time of 1000s to fall through the entire separation column. It is therefore

obvious that experiments with very small particles ($d < 1\mu m$) require a lot of experiment time ($t > 17h$).

B. Horizontal Deflection

Eq. 1 shows that the magnetophoretic force respectively the corresponding horizontal acceleration acting on the particles depends on the diameter. Consequently, larger particles experience higher horizontal accelerations and vice versa. Eq. 6 reveals that the larger the particles, the greater the sinking velocity. These superimposed movements in the horizontal and vertical directions mean that the resulting particle trajectories are independent of particle size. Fig. 11a presents this not very intuitive behavior very nicely.

Fig. 9 shows the horizontal deflection x to be expected for a given coil current I at the level of the entry into the separation zone.

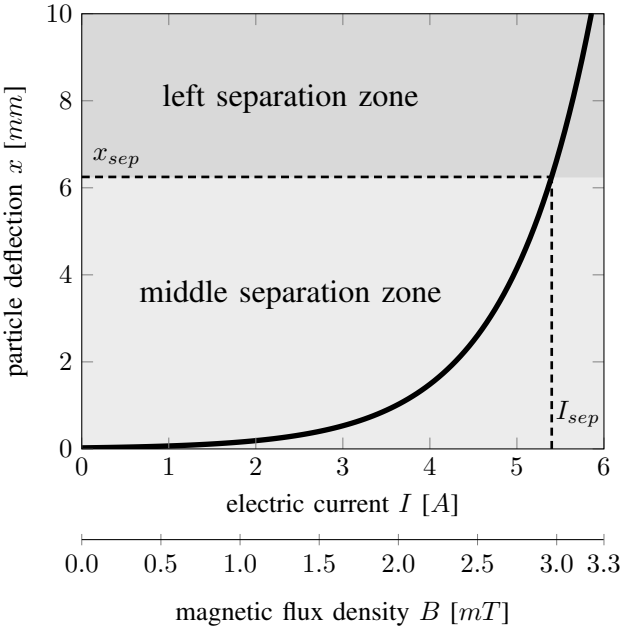

Fig. 9: Magnetic field-dependent horizontal particle deflection.

The second x-axis shows the magnetic flux density B associated with the specified coil current at a selected probe point (*PP*, cf. Fig. 7). With a design-related horizontal deflection of $x_{sep} > 6.25mm$ the particles end up in the left separation zone, with $x_{sep} < 6.25mm$ they end up in the middle zone. The simulations have shown that a current of $I_{sep} \geq 5.41A$ is necessary for a deflection into the left zone.

Consequently, a constant DC magnetic field or fixed coil current over the entire experimental period would result in all particles being deflected identically, which would contradict the desired separation. In order to enable a successful particle separation, the coil current I_{sep} set at the beginning of the simulation ($t = 0s$) must be set to zero exactly when the desired maximum permissible particle diameter has reached the separation zone. As a result, all larger particles that have reached the separation zone by this time end up in the left-hand zone, while all smaller particles arriving after this time are sorted into the middle zone. Fig. 10 presents the separation time t_{sep} to be selected depending on the particle diameter, at which the current must be switched off.

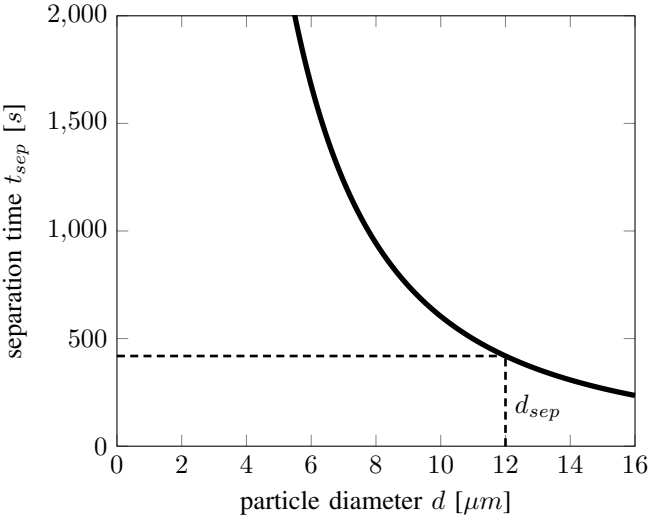

Fig. 10: Diameter-dependent separation time.

In the exemplary simulation case with all particles larger than $d_{sep} > 12\mu m$ are to be separated from the present MnZn ferrite powder, the coil current and thus the magnetic field must be switched off after $t_{sep} = 419s$ (cf. Fig. 10).

Fig. 11 illustrates the time course of the separation process. At the beginning of the simulation, the current I_{sep} is applied to the coil arrays and generates the magnetic field. At the same time, the particles begin to sink in the separation column and are deflected horizontally in the area of the coil arrays. After $t = 235s$, the particle with a diameter of $16\mu m$ reaches the left separation zone (cf. Fig. 11a). This also applies to all subsequent smaller particles up to the specified diameter of $d_{sep} = 12\mu m$ (cf. Fig. 11b). Now the coil current or the magnetic field is switched off at the specified separation time $t_{sep} = 419s$ (cf. Fig. 11c). From this point onwards, there is no further deflection of all subsequent smaller particles due to the disappearance of the magnetic field, so that there is only a purely vertical movement, which then ends in the middle separation zone (cf. Fig. 11d). Finally, it is only necessary to wait until the smallest particles have sunk into the middle zone (cf. Fig. 11e).

The procedure presented here is a very simple type of separation scheme. A finer time-dependent control of the coil current and a variable control of the individual coil arrays can further improve the separation. In addition, it would also be conceivable to realize significantly more compartments in the separation zone in order to achieve a couple of narrower particle size distributions, than merely separating particles that limit the PSD to a specific maximum particle diameter d_{sep}.

The use of AC current control signals and thus the utilization of the frequency-dependent magnetic permeability offer

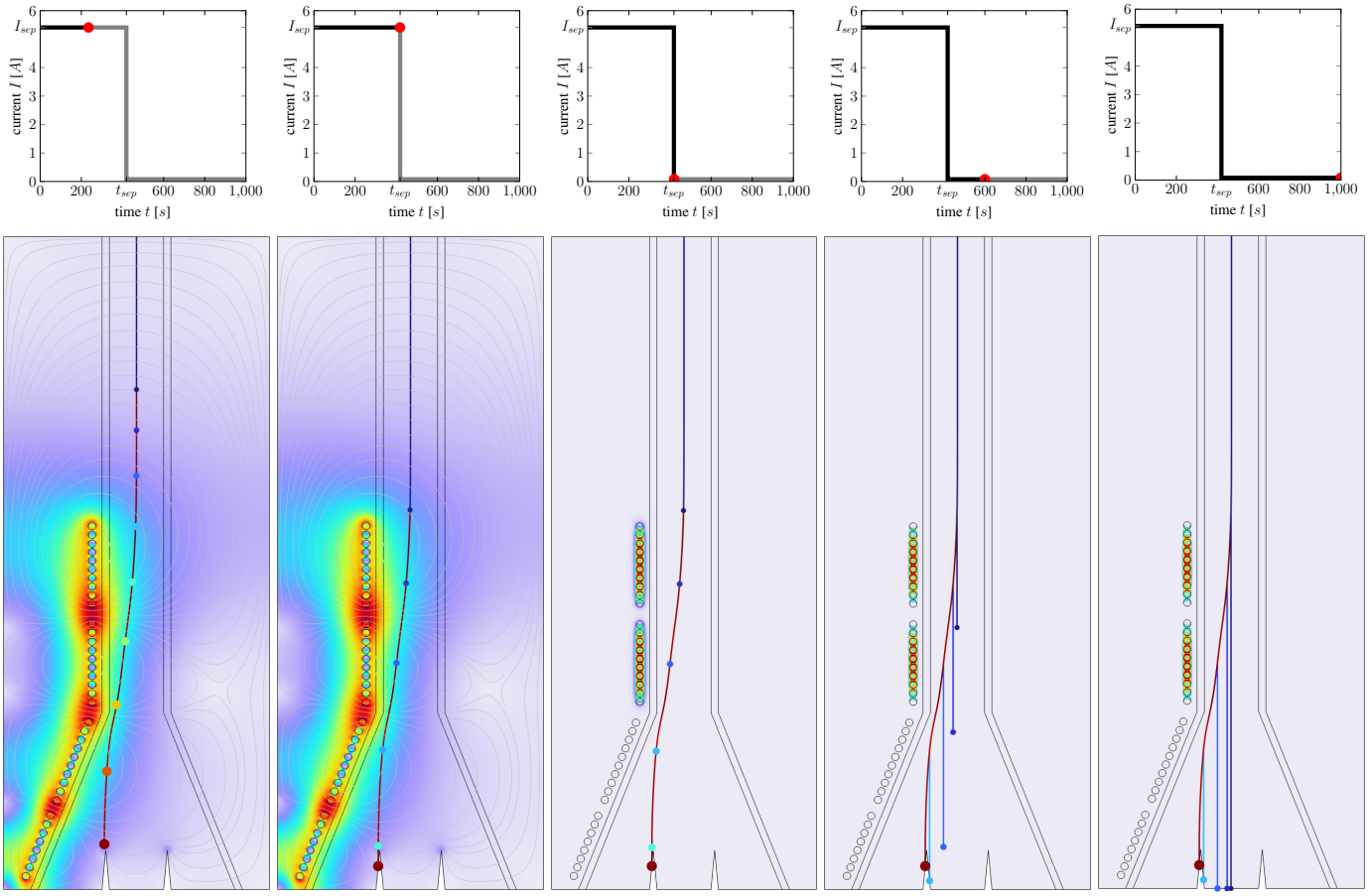

Fig. 11: Particle deflection trajectories of particle diameters ranging from $d = 8\mu m - 16\mu m$ (for $d_{sep} = 12\mu m \rightarrow t_{sep} = 419s$): (a) at $t = 235s$, (b) at $t = t_{sep} - 1s$, (c) at $t = t_{sep} + 1s$, (d) at $t = 600s$, and (e) at $t = 1000s$.

further degrees of freedom. In the field of dielectrophoresis, the previous work by *Kuehne et al.* [7] provides an insight into the frequency-controlled manipulation of particles.

VI. Conclusions and Outlook

The present work demonstrated the fundamentals of magnetophoretic particle separation in a stationary liquid column. First, the particle size distribution of a MnZn ferrite powder and its magnetic permeability were investigated in detail. Simulation results show that in the vertical separation section, particles are successfully separated due to their different sizes. This allows the particles to be deflected horizontally in the magnetic field in time according to a specified size, by the action of the magnetophoretic force.

Further investigations will include, on the one hand, a detailed understanding of efficient control of the coil current. In a second step, the modeling should take into account that the particles are not spherical entities, but deviate relatively strongly from this current assumption. Moreover, the variance of the material characteristic value of the magnetic permeability (often $\pm 20\%$) of the ferromagnetic particles, which is to be expected in practice, must also be evaluated. On the other hand, an experimental setup will be realized to validate the simulation results.

VII. Acknowledgements

Supported by the foundation for promotion of Reinhold Würth University of Heilbronn University of Applied Sciences in Künzelsau. Further thanks to TRIDELTA Weichferrite GmbH for providing the MnZn ferrite powder.

References

[1] N. Pamme, "Continuous flow separations in microfluidic devices," *Lab Chip*, vol. 7, pp. 1644–1659, 12 2007. DOI: 10.1039/B712784G.

[2] P. Sajeesh and A. Sen, "Particle separation and sorting in microfluidic devices: A review," *Microfluidics and Nanofluidics*, vol. 17, pp. 1613–4990, 2014. DOI: 10.1007/s10404-013-1291-9.

[3] R. Rosenweig, *Ferrohydrodynamics*, ser. Cambridge Monographs on Mechanics. Cambridge University Press, 1985, ISBN: 9780521256247.

[4] T. Jones, *Electromechanics of Particles*. Cambridge University Press, 1995, ISBN: 9780521431965.

[5] J. Coey, *Magnetism and Magnetic Materials*, ser. Magnetism and Magnetic Materials. Cambridge University Press, 2010, ISBN: 9780521816144.

[6] TRIDELTA Weichferrite GmbH, *MnZn Ferrite Powder*, 2077, Sep. 2016.

[7] I. Kuehne, N. Philippin, and A. Frey, "Frequency-controlled manipulation of particles in a liquid column based on ac dielectrophoresis," in *COMSOL Conference*, Munich, Germany, 2023.